yield: UV-vis (CH_2Cl_2) λ_{max} (log ϵ) 403 (5.14), 537 (3.88), 571 (4.05), 616 (3.58) nm. Anal. Calcd for $C_{50}H_{55}N_4Cl_4Fe$: C, 66.02; H, 6.09; N, 6.16; Fe, 6.14. Found: C, 65.56; H, 5.91; N, 5.99; Fe, 6.78.

[N^{21},N^{22}-(etheno)TPP]$HClO_4$ (6b), [N-(β-chlorovinyl)-TPP]Co^{II}SCN (13b), and [N-(β-chlorovinyl)TPP]H (14b). (i) Oxidation of (TPP)Co^{II} in the Presence of Acetylene. A CH_2Cl_2 (50 mL) solution of (TPP)Co^{II} (60 mg) was saturated with acetylene gas by bubbling for 1 h under anaerobic conditions. $FeCl_3$ (5.2 equiv) was added at one time. The mixture was vigorously stirred for 1 h at room temperature and then washed with 10% $HClO_4$ and with water twice, successively. Chromatography on silica gel with CH_2Cl_2-acetone (10:1) followed by recrystallization from CH_2Cl_2-hexane afforded **6b** in 66% yield: UV-vis (CH_2Cl_2) λ_{max} (log ϵ) 431 (5.00), 560 (3.97), 600 (3.99), 654 (3.81) nm. Anal. Calcd for $C_{46}H_{31}N_4O_4Cl$: C, 74.74; H, 4.23; N, 7.58. Found: C, 72.58; H, 4.15; N, 7.61.

(ii) Oxidation of (TPP)Co^{II} followed by the Reaction with Acetylene. $FeCl_3$ (4.3 equiv) was added to a CH_2Cl_2 (40 mL) solution of (TPP)Co^{II} (48 mg), and the resulting mixture was stirred for 1.5 h under argon at room temperature to result in the color change to green. Acetylene gas was introduced effectively into this mixture and allowed to react for 3 h. The workup in the same manner as for (i), except that the porphyrin mixture was treated with a saturated NaSCN aqueous solution before chromatographic purification, afforded [N-(β-chlorovinyl)-TPP]Co^{II}SCN (**13b**) in 29% yield together with **6b** (47%). **13b**: ^1H NMR (24 °C) 44.1 (×2), 35.8, -2.9 (8 H, pyrrole β-H), 23.3, 19.6, 2.5, -1.8 (8 H, phenyl o-H), 13.5, 12.2, 7.4, 7.1 (8 H, phenyl m-H), 9.5, 7.6 (4 H, phenyl p-H); UV-vis (CH_2Cl_2) λ_{max} (log ϵ) 447 (5.10), 565 (3.94), 616 (4.05), 666 (3.80) nm. Anal. Calcd for $C_{47}H_{30}N_5SClCo$: C, 71.35; H, 3.82; N, 8.85. Found: C, 71.44; H, 3.70; N, 8.44. The yields of **13b** and **6b** varied in this procedure, and [N-(β-chlorovinyl)TPP]H (**14b**) was isolated from time to time. **13b** was converted into **14b** with trifluoroacetic acid according to Callot's procedure.[6e] **14b**: UV-vis (CH_2Cl_2) λ_{max} (log ϵ) 433 (5.14), 529 (3.84), 569 (4.00), 617 (3.82), 672 (3.60) nm. Anal. Calcd for $C_{46}H_{31}N_4Cl$: C, 81.82; H, 4.63; N, 8.30. Found: C, 79.97; H, 4.25; N, 8.58.

N^{21},N^{22}-Bridged (TPP)$HClO_4$ (7b-11b). $FeCl_3$ (3.5 equiv) was added at one time to a CH_2Cl_2 (50 mL) solution of (TPP)Co^{II} (100 mg) and alkyne (5 equiv), and the whole mixture was stirred vigorously for 1 h. The workup was done according to the procedure for acetylene described above. Although 1-hexyne, propargyl alcohol, phenylacetylene, and diphenylacetylene could be employed to prepare **7b**, **8b**, **9b**, and **11b** in 47, 67, 45, and 44% yield, respectively, 2-butyne-1,4-diol failed to give the corresponding bridged porphyrin **10b**. When $FeCl_3$ was replaced by $Fe(ClO_4)_3 \cdot 6H_2O$ in this procedure, 2-butyne-1,4-diol and diphenylacetylene afforded **10b** and **11b** in 75 and 90% yields, respectively. **7b**: UV-vis (CH_2Cl_2) λ_{max} (log ϵ) 429 (5.08), 559 (3.88), 594 (4.05), 646 (3.79) nm. Anal. Calcd for $C_{50}H_{39}N_4O_4Cl$: C, 75.51; H, 4.94; N, 7.04. Found: C, 74.16; H, 4.82; N, 6.56. **8b**: UV-vis (CH_2Cl_2) λ_{max} (log ϵ) 429 (5.02), 557 (3.85), 595 (3.99), 647 (3.79) nm. Anal. Calcd for $C_{47}H_{33}N_4O_5Cl$: C, 73.80; H, 4.32; N, 7.28. Found: C, 72.20; H, 4.18; N, 6.79. **9b**: UV-vis (CH_2Cl_2) λ_{max} (log ϵ) 429 (5.09), 554 (3.89), 590 (4.02), 640 (3.73) nm. Anal. Calcd for $C_{48}H_{35}N_4O_6Cl$: C, 72.13; H, 4.41; N, 7.01. Found: C, 70.92; H, 4.28; N, 6.57. **10b**: UV-vis (CH_2Cl_2) λ_{max} (log ϵ) 430 (5.08), 561 (3.88), 596 (4.04), 648 (3.83) nm. Anal. Calcd for $C_{52}H_{35}N_4O_4Cl$: C, 76.60; H, 4.33; N, 6.87. Found: C, 76.78; H, 4.27; N, 6.55. **11b**: UV-vis (CH_2Cl_2) λ_{max} (log ϵ) 432 (5.15), 557 (3.93), 593 (4.10), 641 (3.73) nm.

Reaction of Co(III) Porphyrin π Cation Radicals with Diphenylacetylene. (i) Electrochemical Oxidation. (OEP)Co^{II} (40 mg) in 10 mL of CH_2Cl_2 charged in an H-cell was electrolyzed at +1.2 V (vs Ag/AgCl) with stirring and bubbling argon in the presence of TBAP to generate [(OEP)$^{\cdot+}$]$Co^{III}(ClO_4)_2$. After the current was stopped, the electrolyzer was turned off and diphenylacetylene (5 equiv) was added to the solution to result in an immediate color change to green. The solution was stirred for 30 min, evaporated, and chromatographed on silica gel with $CHCl_3$ to give **11a**. As the product could not be separated completely from TBAP, the yield (47%) was calculated with the aid of the visible spectral data of the authentic sample.

(ii) Oxidation with Br_2. Br_2 (29 mg) was added to a mixture of (OEP)Co^{II} (100 mg) and CH_2Cl_2 (20 mL). After the whole mixture was stirred for 1 h at room temperature, diphenylacetylene was added.

(iii) Oxidation of (OEP)Co^{III}Cl. Diphenylacetylene (5 equiv) was added to the mixture of (OEP)Co^{III}Cl (60 mg) and $Fe(ClO_4)_3 \cdot 6H_2O$ (ca. 5 equiv) in CH_2Cl_2 (40 mL). The color of the solution changed immediately, and the ordinary workup afforded **11a** in 50% yield.

Acknowledgment. This work was supported by a Grant-in-Aid for Scientific Research on Priority Area from the Ministry of Education, Science, and Culture of Japan, a Grant for Basic Research from the Inamori Foundation of Japan, and a Grant from the Asahi Glass Research Foundation of Japan. We are grateful to Dr. M. Sato (University of Osaka Prefecture) for the measurement of ESR spectra and to Nichigo Acetylene Co. Ltd. (Osaka, Japan) for the gift of extrapure acetylene gas.

Synthetic and Molecular Orbital Study of η^3(3e)-Butadienyl Complexes of Molybdenum

Brian J. Brisdon,* Robert J. Deeth, Annabelle G. W. Hodson, Christopher M. Kemp, Mary F. Mahon, and Kieran C. Molloy

School of Chemistry, University of Bath, Claverton Down BA2 7AY, U.K.

Received June 22, 1990

Complexes of general formula $MoCl(CO)_2(\eta^3\text{-}CH_2C(CONRR')C{=}CH_2)L_2$ (L_2 = 2,2'-bipyridine, 1,10-phenanthroline) that contain an η^3(3e)-buta-2,3-dienyl ligand are formed by the reaction of $Ph_4P[MoCl(CO)_3L_2]$ with methanolic 1,4-dichlorobut-2-yne in the presence of primary or secondary amines HNRR' (R = H, R' = Me, Et, Pr^n, Ph, $CH_2CH{=}CH_2$, $CH_2C{\equiv}CH$; R = R' = Me, Et, Pr^n). The perfluorocarboxylate complex $Mo(CO)_2(\eta^3\text{-}CH_2C(CONHMe)C{=}CH_2)$(2,2'-bipyridine)($O_2CC_3F_7$) (11), formed by anion exchange, crystallizes in a triclinic space group $P\bar{1}$ with a = 7.440 (3) Å, b = 9.727 (3) Å, c = 17.748 (6) Å, α = 100.58 (3)°, β = 94.84 (2)°, γ = 103.88 (5)°, V = 1214.6 (7) Å^3, and Z = 2; R = 0.064, R_w = 0.072 for 2296 reflections with $I \geq 3\sigma(I)$ having $2 \leq \theta \leq 22°$. An EHMO study of the bonding and potential reactive centers in the ligated η^3-butadienyl ligand is also reported.

Introduction

Factors determining the stereochemistry and reactivity of molybdenum and tungsten(II) complexes of the type $MX(CO)_2(\eta^3\text{-allyl})L_2$ (M = Mo, W, X = halide, and L_2 = bidentate ligand) have been well defined theoretically and experimentally, in order to develop highly regio- and ste-

0276-7333/91/2310-1107$02.50/0

Table I. Yields and Selected Infrared and Analytical Data for $[MoX(CO)_2(\eta^3\text{-}CH_2C(CONRR')C{=}CH_2)L_2]$[a]

R	R′	X	complex, group, yield, %			infrared data,[b] cm^{-1} ν(CO)	ν(C=O) (amide)	ν(NH)	ν(C=C)	anal. found (calc), % C	H	N
Me	Me	Cl	1	A	38	1888, 1960	1612 m		1688 w	48.6 (48.7)	3.8 (3.8)	8.8 (8.9)
Et	Et	Cl	2	A	48	1890, 1958	1608 m		1680 w	50.5 (50.8)	4.4 (4.4)	8.3 (8.4)
Et	Et	Cl	3	A	43	1876, 1960	1615 m		1679 w	53.7 (53.1)	4.3 (4.2)	8.2 (8.1)
Pr^n	Pr^n	Cl	4	B	40	1885, 1970	1630 m		1666 w	49.3 (52.7)	4.1 (4.9)	7.2 (8.0)
H	Me	Cl	5	A	59	1880, 1955	1615 m	3432 w	1672 w	46.9 (47.6)	3.2 (3.5)	8.5 (9.2)
H	Et	Cl	6	A	72	1889, 1963	1651 m	3320 w	1670 w	48.2 (48.7)	3.9 (3.8)	8.2 (8.9)
H	Pr^n	Cl	7	A	48	1880, 1957	1648 m	3401 w	1675 w	49.4 (49.8)	4.5 (4.1)	8.2 (8.7)
H	Ph	Cl	8	B	71	1880, 1960	1662 m	3374 w	1671 w	54.0 (53.5)	4.1 (3.4)	7.3 (8.1)
H	$CH_2CH{=}CH_2$	Cl	9	B	87	1881, 1958	1639 m	3402 w	1678 w	50.1 (50.0)	3.5 (3.7)	8.2 (8.7)
H	$CH_2C{\equiv}CH$	Cl	10	B	72	1882, 1958	1654 m	3412 w	1680 w	50.2 (50.2)	3.3 (3.4)	8.4 (8.7)
H	Me	$C_3F_7CO_2$	11		63	1898, 1976	1658 m	3440 w	1664 sh	41.1 (41.8)	2.5 (2.5)	6.5 (6.6)
H	Et	$C_3F_7CO_2$	12		75	1897, 1973	1649 m	3412 w	1672 sh	42.3 (42.7)	2.6 (2.7)	6.7 (6.5)
H	Pr^n	$C_3F_7CO_2$	13		56	1899, 1969	1648 m	3403 w	1677 sh	43.2 (43.7)	3.0 (3.0)	6.3 (6.4)
H	Ph	$C_3F_7CO_2$	14		61	1898, 1973	1658 m	3380 w	c	46.8 (46.7)	2.7 (2.5)	5.9 (6.0)
H	$CH_2CH{=}CH_2$	$C_3F_7CO_2$	15		54	1898, 1970	1640 m	3401 w	1680 sh	43.3 (43.8)	2.9 (2.7)	6.2 (6.3)

[a] L_2 = bpy, except for 3 where L_2 = phen. [b] As Nujol mulls; all bands strong unless otherwise stated. [c] Not observed.

reospecific stoichiometric and catalytic allylic alkylation and coupling reactions.[1-6] However, little attempt has been made to explore possible new and stereoselective routes to C–C bond formation by exploiting the extreme facility and high efficiency of the $[MX(CO)_3L_2]^-$ anion in undergoing oxidative addition with unsaturated organic substrates to generate these formally seven-coordinate, 18-electron products containing an η^3-allyl ligand or its 3-electron donor equivalent.[7] In the first of a series of papers on this theme, we showed that the molybdenum-coordinated 4-methoxy-4-oxobut-2-en-2-yl-C^2O moiety could be generated via the reaction of $[MoCl(CO)_3bpy]^-$ (bpy = 2,2′-bipyridine) with propargyl chloride under the appropriate conditions.[8]

More recently in a preliminary publication, we reported the use of the same carbonylate anion to generate novel monosubstituted η^3-butadienyl (A) and a trisubstituted η^3-allyl (B) species by reaction with 1,4-dichlorobut-2-yne

$$Ph_4P[MoCl(CO)_3bpy] + ClCH_2C{\equiv}CCH_2Cl \xrightarrow{MeOH} \underset{A}{MoCl(CO)_2bpy(\eta^3\text{-}CH_2C(CO_2Me)C{=}CH_2)} + \underset{B}{MoCl(CO)_2bpy(\eta^3\text{-}CH_2C(CO_2Me)C(OMe)Me)}$$

in the presence of methanol.[9] (The positions of the hydrogen atoms on the η^3-ligand could not be defined, so that we were unable to differentiate between an η^3-buta-1,3-dienyl and a buta-2,3-dienyl formulation for the $CH_2C(CO_2Me)C{=}CH_2$ ligand. For reasons described in this paper we consider the latter more appropriate.)

It was also shown that in alcohol–amine mixtures, alkylamido-substituted η^3-butadienyl analogues of A were formed.[10] In this paper we have sought to define the limits of this reaction for primary and secondary amines and we have analyzed theoretically the mode of bonding and potential reaction centers of the η^3-butadienyl ligand.

Results and Discussion

It has been shown that in the reaction of $[MoCl(CO)_3bpy]^-$ with 1,4-dichlorobut-2-yne in methanol, the reaction pathway is strongly influenced by the presence of water, which promotes the formation of the η^3-butadienyl complex $MoCl(CO)_2(\eta^3\text{-}CH_2C(CO_2Me)C{=}CH_2)bpy$ as the only major metal-containing product.[9] The same product is formed if a tertiary amine such as trimethylamine or pyridine is present in the reaction mixture in place of water. However, if the reaction is carried out in the presence of certain primary or secondary amines, orange, microcrystalline solids of general formula $MoCl(CO)_2(\eta^3\text{-}CH_2C(CONRR')C{=}CH_2)bpy$ (R = H, R′ = Me, Et, Pr^n, Ph, $CH_2CH{=}CH_2$, $CH_2C{\equiv}CH$; R = R′ = Me, Et or Pr^n) are formed.

An analogous reaction occurs between $[MoCl(CO)_3phen]^-$ (phen = 1,10-phenanthroline) and 1,4-dichlorobut-2-yne in methanolic diethylamine solution, with the solubilities of all the products being generally low but somewhat dependent upon the nature of the amine substituents R and R′. Representative examples of this class of η^3-butadienyl complexes were converted into the more soluble perfluorocarboxylate derivatives by reaction with $AgBF_4$ in acetone solutions of $NaO_2CC_3F_7$. This resulted in precipitation of AgCl and the formation of solutions of the complexes $Mo(CO)_2(\eta^3\text{-}CH_2C(CONHR')C{=}CH_2)(bpy)(O_2CC_3F_7)$ (R′ = Me, Et, Pr^n, Ph, $CH_2CH{=}CH_2$), which were readily isolated as orange crystalline solids. Yields and analytical and selected infrared data for these complexes are summarized in Table I.

Spectral Data. Infrared spectra were dominated by the pair of carbonyl modes expected for a pseudooctahedral complex containing *cis*-dicarbonyls. Absorptions due to the amide carbonyl group were found at slightly higher wavenumbers than values typical for carbamoyl complexes.[11] Complexes **5–15** prepared from primary amines exhibited a weak, sharp ν(N—H) mode near 3400 cm^{-1}, and complex **10** derived from propargylamine exhibited additional weak sharp absorptions at ca. 3300 and 2190 cm^{-1} (the latter being Raman active only) caused by ν(CH) and ν(C≡C) stretching modes of the –C≡CH moiety. Replacement at the metal center of Cl^- by $C_3F_7CO_2^-$ resulted in little change in ν(N—H) or ν(C=O) values, but both

(1) Curtis, M. D.; Eisenstein, O. *Organometallics* **1984**, *3*, 887.
(2) Trost, B. M.; Lautens, M. *J. Am. Chem. Soc.* **1987**, *109*, 1469.
(3) Trost, B. M.; Hung, M. H. *J. Am. Chem. Soc.* **1983**, *105*, 7757.
(4) Trost, B. M.; Tametski, G. B.; Hung, M. H. *J. Am. Chem. Soc.* **1987**, *109*, 2176.
(5) Trost, B. M.; Merlic, C. A. *J. Am. Chem. Soc.* **1990**, *112*, 9590.
(6) Brisdon, B. J.; Brown, D. W.; Willis, C. R. *Polyhedron* **1986**, *5*, 439.
(7) Brisdon, B. J.; Edwards, D. A.; White, J. W. *J. Organomet. Chem.* **1978**, *156*, 427.
(8) Brisdon, B. J.; Brown, D. W.; Willis, C. R.; Drew, M. G. B. *J. Chem. Soc., Dalton Trans.* **1986**, 2405.
(9) Drew, M. G. B.; Brisdon, B. J.; Brown, D. W.; Willis, C. R. *J. Chem. Soc., Chem. Commun.* **1986**, 1510.
(10) Brisdon, B. J.; Hodson, A. G. W.; Mahon, M. F.; Molloy, C. M. *J. Organomet. Chem.* **1988**, *344*, C8.
(11) Ford, P. C.; Rokicki, A. *Adv. Organomet. Chem.* **1988**, *28*, 139.

Table II. ^{1}H and ^{13}C NMR Data[a] for $MoX(CO)_2(\eta^3\text{-}CH_2C(CONRR')C{=}CH_2)L_2$

complex	H^{11}_a, H^{11}_s, C^{11}	H^{14}_a, H^{14}_s, C^{14}	C^{12}, C^{13}, C^{15}	aliphatic NRR' ^{1}H	aliphatic NRR' ^{13}C	aromatic ^{1}H	aromatic ^{13}C	NH	CO
1	1.87 (s), 3.51 (s), 50.7	5.55 (d, 2.4), 6.14 (d, 2.4), 104.2	60.9, 169.1, 175.3	2.24 (3 H), 2.93 (3 H)	36.6 (CH_3), 39.3 (CH_3)	7.42, 7.47, 7.97, 6.04, 8.77, 8.83	125.4, 125.9, 139.1, 139.2, 151.8, 152.1		220.7, 221.6
2	1.89 (s), 3.46 (s), 49.6	6.10 (s, 2.4), 6.25 (d, 2.0), 102.7	60.9, 168.2, 174.9	0.53 (t, 6.4, 3 H), 2.79 (m, 2 H), 1.06 (t, 6.4, 3 H), 3.17 (m, H), 3.77 (m, H)	11.2 (CH_3), 42.3 (CH_2)	7.43, 7.47, 7.98, 8.06, 8.80, 8.85	125.0, 125.5, 138.6, 139.1, 151.9, 152.7		220.7, 221.4
3	1.89 (s), 3.71 (s), 50.1	5.62 (d, 2.2), 6.18 (d, 2.4), 103.4	60.2, 168.2, 175.2	0.00 (m, 3 H), 0.94 (s, 3 H), 2.23 (m, H), 2.38 (m, H), 2.78 (m, H), 3.68 (m, H)	12.4 (CH_3), 40.9 (CH_2)	7.75, 7.87, 8.43, 8.46	124.5, 124.8, 127.3, 127.4, 130.1, 130.2, 138.2, 138.4, 151.6, 151.9		220.7, 221.4
4	1.97 (s), 3.37 (s), 49.3	5.49 (d, 2.4), 6.08 (d, 2.4), 102.3	62.0, 168.8, 175.3	0.47 (t, 7.1, 3 H), 0.84 (m, 2 H), 0.98 (t, 7.1, 3 H), 1.49 (m, H), 1.86 (m, H), 2.73 (m, H), 2.84 (m, H), 3.34 (m, H), 3.60 (m, H)	11.0 (CH_3), 19.5 (CH_2), 47.7 (CH_2)	7.43, 7.48, 7.97, 8.08, 8.78, 8.82	125.1, 125.5, 138.6, 138.9, 151.2, 151.5		220.4, 221.5
11	1.96 (s), 3.96 (s), 52.6	5.79 (d, 2.2), 6.30 (d, 2.2), 106.1	c, 166.3, 176.4	1.99 (d, 5.0, 3 H)	26.1 (CH_3)	7.51, 7.57, 8.05, 8.83, 8.94	126.3, 126.6, 139.8, 152.3, 152.3, 152.7	5.31 (q, 5.0, H)	219.9, 222.7
12	1.96 (s), 3.98 (s), 52.2	5.80 (d, 2.2), 6.32 (d, 2.2), 105.6	57.5, 166.2, 175.9	0.52 (t, 7.2, 3 H), 2.28 (m, H), 2.66 (m, H)	14.2 (CH_3), 34.2 (CH_2)	7.53, 7.56, 8.07, 8.84, 8.93	126.0, 126.2, 139.6, 139.9, 152.3, 153.2	5.32 (t, 5.0, H)	218.5, 220.6
13	1.96 (s), 3.99 (s), b	5.79 (d, 2.2), 6.31 (d, 2.2), 105.8	58.0, 166.4, 176.3	0.62 (t, 7.8, 3 H), 0.92 (m, 7.8, 2 H), 2.07 (m, 6.8, H), 2.63 (m, 7.4, H)	11.4 (CH_3), 22.7 (CH_2), 41.4 (CH_2)	7.52, 7.55, 8.09, 8.84, 8.92	126.3, 126.5, 139.9, 140.2, 152.1, 152.6	5.45 (t, 5.0, H)	218.9, 220.6
14	2.03 (s), 4.06 (s), 51.7	5.92 (d, 2.4), 6.48 (d, 2.2), 106.4	57.8, 164.6, 176.8			7.45, 7.57, 7.89, 8.02, 8.88, 8.90	126.1, 126.4, 139.6, 152.3, 152.3, 152.2	b	218.0, 219.7
15	1.97 (s), 3.99 (s), 52.2	5.80 (d, 2.2), 6.33 (d, 2.4), 105.8	57.4, 166.2, 175.8	2.73 (m, H), 3.31 (m, H), 4.86 (m, 2 H), 5.22 (m, H)	41.8 (CH_2), 134.5 (CH), c	7.58, 7.61, 7.91, 8.08, 8.85, 8.91	126.1, 126.3, 139.7, 140.0, 151.9, 152.3	5.47 (t, 5.0, H)	218.9, 220.1

[a] In CD_2Cl_2 at room temperature; in ppm (multiplicity, J in Hz). [b] Partially obscured by CD_2Cl_2 signal. [c] Not observed.

ν(C≡O) modes were shifted by ca. 15 cm^{-1} to higher wavenumbers, reflecting the differing electronegativities of these anions. ^{1}H and ^{13}C NMR spectra for perfluorocarboxylate complexes 11–15 and, where possible, chloro complexes were recorded in CD_2Cl_2, and pertinent data are presented in Table II. Spectra of representative examples of these complexes were temperature invariant over the range +25 to −80 °C. The uncoordinated C=CH_2 moiety of the π-enyl ligand resonates in the ^{1}H NMR spectrum as two doublets centered between 5.4 and 6.5 ppm with average coupling constants of 2.2 Hz. Very similar data have been reported recently[12] for $Mo(CO)_2(\eta\text{-}C_5Me_5)(\eta^3\text{-}CH_2CHC{=}CH_2)$ formed by desilylation of $[Mo(CO)_2(\eta^4\text{-}CH_2{=}CHC(SiEt_3){=}CH_2)(\eta^5\text{-}C_5Me_5)][BF_4]$. Singlets near 3.9 and 1.9 ppm were attributed to the syn and anti protons, respectively, of the terminal unsubstituted allyl methylene residue, and NH proton resonances were in general observed at ca. 5.5 ppm as broad triplets with coupling constants of ~5 Hz. Although the methyl group in the *E*-methylamido substituent of $Mo(CO)_2(\eta^3\text{-}CH_2C(CONHMe)C{=}CH_2)(bpy)(O_2CC_3F_7)$ does not appear to be greatly affected by the magnetic anisotropic effect of the bpy ligand, both the methyl and methylene protons of the analogous ethyl derivative **12** suffer an upfield shift, and in addition two signals are observed for the latter protons, which are rendered inequivalent by the chirality of the metal-coordinated η^3-butadienyl system. A similar effect is also observed in the spectrum of complex **13** (Figure 1) derived from *n*-propylamine, and progressively more complex spectra were observed for the methylene signals of -$CONEt_2$ and -$CONPr^n_2$ containing derivatives **2**–**4**. In several cases signals arising from the solvent in the 54 ppm region prevented complete spectral assignments of ^{13}C NMR data, but in general the spectra for the η^3-ligand, which are summarized in Table II, are similar to those reported previously.[9,12]

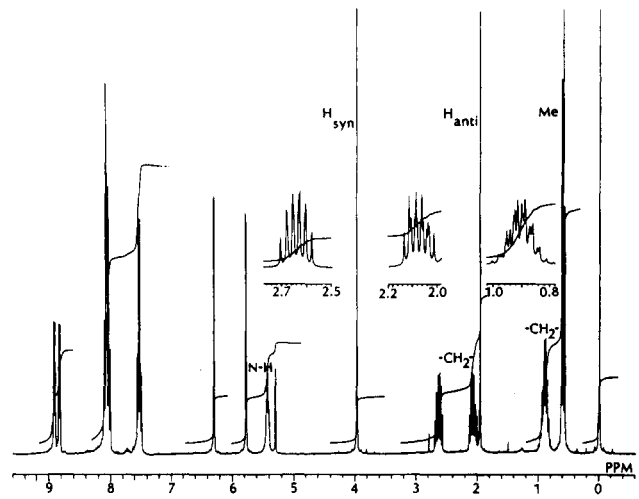

Figure 1. ^{1}H NMR spectrum of $Mo(CO)_2(\eta^3\text{-}CH_2C(CONHPr)C{=}CH_2)bpy(O_2CC_3F_7)$ (**13**).

In order to investigate the effect that the steric and electronic properties of primary and secondary amines might have on the reaction described above, the reaction of $[MoCl(CO)_3bpy]^-$ with $ClCH_2C{\equiv}CCH_2Cl$ in methanol was carried out in the presence of one or more primary or secondary amines having pK_a values for their conjugate acids ranging from 4.6 to 11.0. In each reaction a single major product was formed, as indicated in Table III. The results of these competition experiments indicate that for sterically small amines (R, R' = Me, Et) the relative basicities of the amines are important in determining the reaction product. However, isolation of only compound

(12) Benyunes, S. A.; Green, M.; McPartlin, M.; Nation, C. B. M. *J. Chem. Soc., Chem. Commun.* **1989**, 1881.

Table III. Reaction Products from $[MoCl(CO)_3bpy]^-$ and $ClCH_2C{\equiv}CCH_2Cl$ in Methanol–Amine Mixtures

amine	pK_a[a]	other reactants	η^3-butadienyl substituent –C(O)R
H_2NMe	10.66		–HNMe
H_2NMe	10.66	$HNMe_2$	$-NMe_2$
$HNMe_2$	10.73	H_2NPr^n	$-HNPr^n$
$HNMe_2$	10.73		$-NMe_2$
H_2NEt	10.81		–HNEt
H_2NEt	10.81	$HNEt_2$	–HNEt
$HNEt_2$	10.49		$-NEt_2$
H_2NPr^n	10.71		$-HNPr^n$
$HNPr^n_2$	10.71	H_2O	$-NPr^n_2$
$H_2NCH_2CH{=}CH_2$	9.50	H_2O	$-HNCH_2CH{=}CH_2$
$H_2NCH_2C{\equiv}CH$	8.15	H_2O	$-HNCH_2C{\equiv}CH$
H_2NPr^i	10.63	H_2O	–OMe
$HNPr^i_2$	10.91	H_2O	–OMe
$HNPh_2$	5.12	H_2O	–OMe
H_2NPr^i	10.63	$HNPr^i_2$	*b*
H_2NPr^i	10.63		*b*
$HNPr^i_2$	10.91		*b*
H_2NPh	4.63	H_2O	–HNPh

[a] pK_a of amine conjugate acid (*Handbook of Chemistry and Physics*, 64 ed.; CRC Press: Boca Raton, FL, 1984; D-164). [b] $MoCl(CO)_2(bpy)(\eta^3\text{-}CH_2C(CO_2Me)C(OMe)Me)$.

Table IV. Crystal Data for $C_{22}F_7H_{16}MoN_3O_5$ (11)

formula	$C_{22}F_7H_{16}MoN_3O_5$
fw	631.3
space group	$P\bar{1}$
a, Å	7.440 (3)
b, Å	9.727 (9)
c, Å	17.748 (6)
α, deg	100.58 (3)
β, deg	94.84 (2)
γ, deg	103.88 (5)
V, Å^3	1214.67
μ(Mo Kα), cm^{-1}	5.49
λ(Mo Kα), Å	0.710 69
ρ(calcd), g cm^{-3}	1.73
Z	2
no. of reflns collcd	3355
no. of data $I > 3\sigma(I)$	2296
no. of variables	288
quadrant collcd	$+h,\pm k,\pm l$
F(000)	628
T, K	298
R	6.38
R_w	7.23

13 from reactions carried out in the presence of mixtures of $HNMe_2$ and H_2NPr^n (pK_a 10.73 and 10.71, respectively) show that steric factors predominate for reactions involving a mixture of amines with similar basicities. It is also interesting to note that larger amines (R = H, R′ = Ph, $CH_2CH{=}CH_2$, $CH_2C{\equiv}CH$; R = R′ = Pr^n) will only react with $[MoCl(CO)_3bpy]^-$ in the presence of a small donor such as water or another amine. For even longer chain or more bulky primary (R = H, R′ = Pr^i) or secondary (R = R′ = Pr^i, Ph) amines, alkoxycarbonylated complexes[9] were formed by reaction with MeOH rather than the amine.

Crystal Structure Determination. A solid-state crystal structure determination of $Mo(CO)_2(\eta^3\text{-}CH_2C(CONHMe)C{=}CH_2)(bpy)(O_2CC_3F_7)$ (11) was carried out in order to define the stereochemistry of the unusual η^3-butadienyl group and provide a basis for a theoretical study. In addition, no crystallographic studies on molybdenum or tungsten heptafluorobutyrate derivatives appear to have been recorded, and consequently data on this ligand are also briefly reported. A preliminary report on this structure has been communicated.[10]

Figure 2 shows an ORTEP view of the molecule and the atomic numbering scheme used. Fractional coordinates are given in Table V and important interatomic parameters in Table VI. The central molybdenum atom can be described as heptacoordinate, being bonded to the two nitrogen atoms of 2,2′-bipyridyl [Mo–N(1), 2.224 (8) Å; Mo–N(2), 2.247 (8) Å], two carbonyl groups [Mo–C(17), 1.971 (13) Å; Mo–C(18), 1.975 (13) Å], a monodentate $C_3F_7CO_2$ group, and a bidentate, substituted η^3-butadienyl system C_6H_8NO. The carbonyl groups are mutually cis with the C(17)–Mo–C(18) bond angle of 82.1 (5)° comparing well with the value of 84 (2)° predicted from infrared ν(CO) solution intensity measurements. Both metal–carbonyl groups are essentially linear [Mo–C(17)–O(2), 178.1 (1.1)°; Mo–C(18)–O(3), 176.5 (1.4)°], and the metal–carbon and C–O carbonyl bond lengths [C(17)–O(2),

Table V. Fractional Atomic Coordinates and Thermal Parameters (Å^2) for 11

atom	*x*	*y*	*z*	U_{iso}[a]
Mo	–0.07060 (14)	0.43341 (8)	0.18086 (4)	0.0414 (6)*
O(1)	1.1694 (14)	0.1339 (9)	0.1156 (5)	0.072 (6)*
O(2)	0.6154 (15)	0.5591 (9)	0.1144 (6)	0.091 (7)
O(3)	1.1915 (17)	0.7307 (9)	0.1683 (6)	0.086 (7)*
O(4)	0.8968 (12)	0.5291 (7)	0.2964 (4)	0.055 (5)*
O(5)	0.8476 (25)	0.7420 (11)	0.2871 (7)	0.136 (11)*
N(1)	0.7641 (13)	0.2405 (8)	0.2179 (4)	0.042 (5)*
N(2)	1.1345 (13)	0.3590 (8)	0.2534 (4)	0.043 (5)*
N(3)	0.8615 (15)	0.0283 (9)	0.0799 (5)	0.054 (6)*
C(11)	1.1286 (21)	0.4073 (11)	0.0891 (6)	0.060 (8)*
C(12)	0.9806 (18)	0.2805 (11)	0.0796 (5)	0.052 (7)*
C(13)	0.8052 (18)	0.3061 (11)	0.0646 (6)	0.053 (7)*
C(14)	0.6498 (24)	0.2607 (15)	0.0136 (7)	0.079 (9)*
C(15)	1.0151 (20)	0.1422 (12)	0.0935 (5)	0.055 (7)*
C(16)	0.8764 (25)	–0.1112 (12)	0.0937 (7)	0.081 (9)*
C(17)	0.7316 (17)	0.5140 (11)	0.1402 (6)	0.052 (7)*
C(18)	1.0896 (22)	0.6225 (13)	0.1726 (6)	0.065 (8)*
C(19)	0.8805 (23)	0.6571 (14)	0.3216 (7)	0.072 (9)*
C(20)	0.9172 (26)	0.7005 (14)	0.4114 (9)	0.083 (11)*
C(22)	1.2753 (40)	0.7993 (35)	0.4293 (12)	0.147 (23)*
F(1)	0.8763 (24)	0.8220 (14)	0.4352 (6)	0.167 (12)*
F(2)	0.8200 (19)	0.6011 (13)	0.4419 (5)	0.126 (9)*
F(3)	1.1635 (23)	0.5799 (11)	0.4378 (6)	0.159 (11)*
F(4)	1.1270 (25)	0.7606 (16)	0.5303 (4)	0.174 (12)*
F(5)	1.2791 (19)	0.7617 (15)	0.3551 (6)	0.145 (11)*
F(6)	1.4279 (20)	0.8146 (20)	0.4716 (9)	0.179 (13)*
F(7)	1.2352 (36)	0.9431 (13)	0.4409 (11)	0.235 (19)*
C(1)	0.5818 (17)	0.1748 (11)	0.1921 (5)	0.049 (2)
C(2)	0.4873 (21)	0.0526 (12)	0.2105 (6)	0.065 (3)
C(3)	0.5870 (22)	–0.0146 (14)	0.2568 (7)	0.073 (3)
C(4)	0.7688 (18)	0.0488 (12)	0.2840 (6)	0.057 (3)
C(5)	0.8576 (16)	0.1770 (10)	0.2630 (5)	0.043 (2)
C(6)	1.0577 (16)	0.2502 (10)	0.2878 (5)	0.043 (2)
C(7)	1.1638 (21)	0.2060 (13)	0.3428 (7)	0.069 (3)
C(8)	1.3523 (24)	0.2781 (15)	0.3600 (8)	0.084 (4)
C(9)	1.4267 (24)	0.3897 (14)	0.3264 (7)	0.075 (4)
C(10)	1.3079 (19)	0.4261 (12)	0.2743 (6)	0.056 (3)
C(21)	1.1181 (35)	0.7159 (22)	0.4524 (11)	0.115 (6)

[a] Asterisk represents U_{eq} values.

Table VI. Interatomic Distances (Å) and Angles (deg) with Standard Deviations in Parentheses for $Mo(CO)_2(\eta^3\text{-}CH_2C(CONHMe)C{=}CH_2)(bpy)(O_2CC_3F_7)$

Mo–O(4)	2.150 (7)	Mo–N(1)	2.224 (8)
Mo–N(2)	2.247 (8)	Mo–C(11)	2.314 (13)
Mo–C(12)	2.235 (10)	Mo–C(13)	2.200 (10)
Mo–C(17)	1.971 (13)	Mo–C(18)	1.975 (13)
O(2)–C(17)	1.157 (14)	O(3)–C(18)	1.160 (15)
N(3)–C(16)	1.451 (14)	N(3)–C(15)	1.357 (16)
C(11)–C(12)	1.416 (17)	C(12)–C(13)	1.399 (18)
C(13)–C(14)	1.335 (18)	C(12)–C(15)	1.487 (16)
O(1)–C(15)	1.208 (16)		
C(12)–Mo–C(11)	36.2 (4)	C(13)–C(12)–C(11)	112.5 (10)
C(13)–Mo–C(12)	36.8 (4)	C(13)–Mo–C(11)	62.4 (5)
O(2)–C(17)–Mo	178 (1)	C(18)–Mo–C(17)	82.1 (5)
C(19)–O(4)–Mo	127.9 (7)	O(3)–C(18)–Mo	176.0 (10)
		O(5)–C(19)–O(4)	129.0 (10)

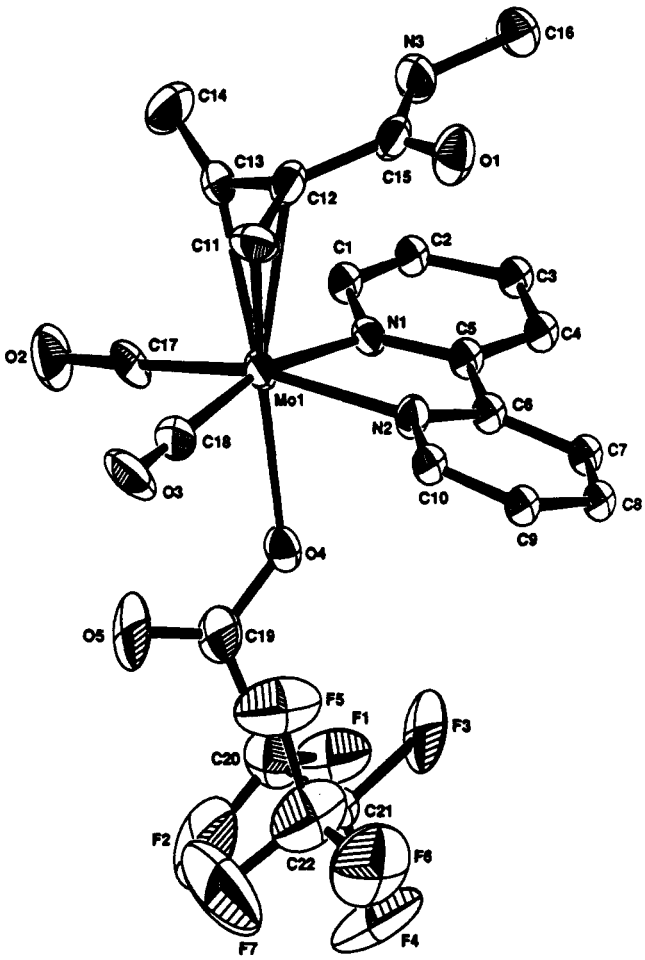

Figure 2. ORTEP plot of $Mo(CO)_2(\eta^3\text{-}CH_2C(CONHMe)C{=}CH_2)(2,2'\text{-bipyridine})(O_2CC_3F_7)$ (11) with atom-labeling scheme and 33% ellipsoids.

1.157 (14) Å; C(18)–O(3), 1.160 (15) Å] are unexceptional. Parameters associated with the two bipyridyl rings compare well with values found for related $MoX(CO)_2(\eta^3$-allyl)bpy structures,[8,9,13] and the rings of the bpy unit are both planar within experimental error, but the crowded metal coordination site is reflected in a slight distortion of the bpy plane with the two rings intersecting at an angle of 9.6°. No structure determinations of heptafluorobutyrate complexes are available for direct comparison of bond lengths, but consideration of the relative bond lengths and angles of Mo–O(4) [2.150 (7) Å] and Mo–O(5) [3.454 Å], and the O(4)–C(19)–O(5) and Mo–O(4)–C(19) bond angles of 129.5 (12) and 127.9 (7)°, respectively, confirms the expected monodentate coordination mode. The C_3F_7 fragment in this molecule is slightly disordered. This is evidenced by the relatively large error in the C–F bond lengths and thermal parameters for all atoms contained therein (see Table S3, supplementary material). However, the very low positional disorder of approximately 5% in the region of the fluorine atoms did not extend to the carbon backbone and hence was not modeled. The C_3F_7 unit itself consists of a chain of three carbon atoms [C(20)–C(21)–C(22), 118.2 (15)°] with the CF_3 and two CF_2 groups in a staggered conformation. Dihedral angles within these groups are within the ranges 53–63 and 163–177°.

The bond lengths and angles associated with the carbon skeleton of the η^3-$CH_2C(CONHMe)C{=}CH_2$ ligand are similar to those in molybdenum-bound η^3-$CH_2C(CO_2Me)C{=}CH_2$ and η^3-$CH_2CHC{=}CH_2$ ligands.[9,12] The Mo–C(11) and Mo–C(12) distances of 2.314 (13) and 2.235 (10) Å, respectively, and the C(11)–C(12) and C(12)–C(13) separations of 1.416 (17) and 1.399 (18) Å plus a C(11)–C(12)–C(13) angle of 112.5 (10)° are typical of parameters found in substituted η^3-allyl complexes of molybdenum.[14] However, the Mo–C(13) separation at 2.200 (10) Å is noticeably shorter than that normally observed between Mo and the terminus of an allyl system. The fourth carbon atom C(14) of the butadienyl system is bent away from molybdenum and at a distance of 3.378 (12) Å is considered to be nonbonded to the metal center. The methyl and carbonyl groups of the –CONHMe substituent are oriented away from the terminal $C{=}CH_2$ moiety, and the dihedral angle C(16)–N(3)–C(15)–O(1) of -0.7° shows that this portion of the C_6H_8NO ligand is almost planar, with the Me group located well above the bpy plane [e.g. C(16)–C(4), 3.70 (1) Å]. Thus the ligand may be derived from a 2-substituted η^3-allyl system by substituting a double bond onto one terminus of the allyl ligand. The uncoordinated double bond of the η^3-butadienyl moiety can then be defined at the extremes as being either conjugated or unconjugated with the η^3-allyl function, according to the positions of the hydrogen atoms on the terminal carbon C(14). Thus if these hydrogen atoms lie in the plane of the allyl system, the double bond is highly conjugated and the ligand is best regarded as a buta-1,3-dienyl system (I).

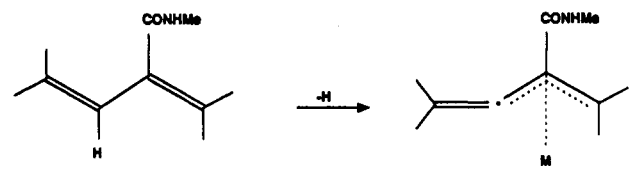

I

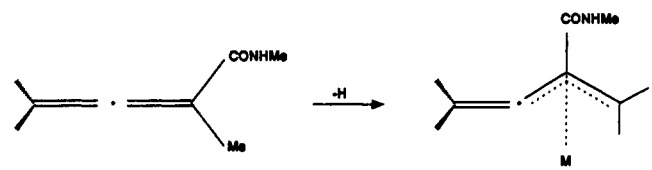

II

If the hydrogen atoms are orthogonal to the plane of the allyl system, the terminal double bond is not conjugated and the ligand can be derived from a buta-2,3-dienyl system as is illustrated in II. Since the C(13)–C(14) bond length in 11 of 1.335 (18) Å is similar to the terminal bond length in free butadiene[15] and is also within the range found for the uncoordinated $C{=}CH_2$ of a ligated allene species,[16] it is not diagnostic of either arrangement.

The position of the hydrogen atoms of the butadienyl ligand in 11 could not be determined directly, and hence to explore further the bonding in this species and to determine potential reactive centers in this unusual ligand, a theoretical study of the system was undertaken.

Theoretical Studies. A d^4 ML_5 fragment is isolobal with CH^+; therefore in an unsubstituted allyl the $ML_5(\eta^3\text{-}C_3H_5)$ group is isolobal with $(CH^+)(C_3H_5^-)$ or bicyclobutane. There should be no barrier to rotation of the $C_3H_5^-$ fragment about the isolobal CH^+ group, and hence it is expected and found[1] that only a relatively small, second-

(13) Fenn, R. H.; Graham, A. J. *J. Organomet. Chem.* **1972**, *37*, 137. Drew, M. G. B.; Brisdon, B. J.; Day, A. *J. Chem. Soc., Dalton Trans.* **1981**, 1310.

(14) Murrall, N. W.; Welch, A. J. *J. Organomet. Chem.* **1986**, *301*, 109.

(15) Aten, C. E.; Hedberg, L.; Hedberg, K. *J. Am. Chem. Soc.* **1968**, *90*, 2463.

(16) Otsuka, S.; Nakamura, A. *Adv. Organomet. Chem.* **1976**, *14*, 245.

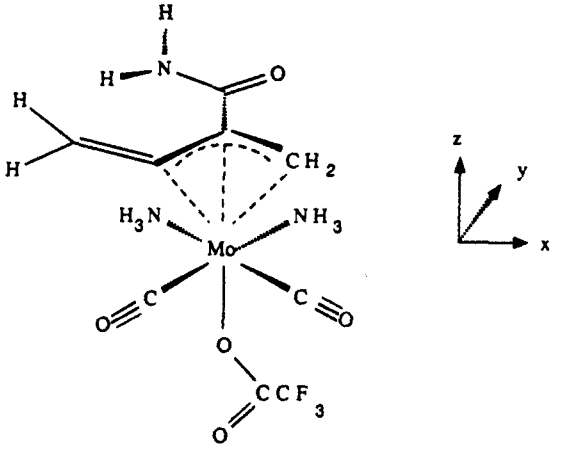

Figure 3. Model complex $Mo(CO)_2(\eta^3\text{-}CH_2C(CONH_2)C{=}CH_2)(NH_3)_2(O_2CCF_3)$. See text for details of bond lengths and angles.

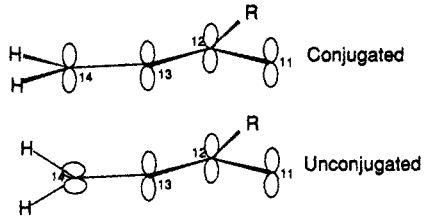

Figure 4. Extreme orientations of the C(14) pπ orbital in the η^3-butadienyl ligand.

order effect is responsible for the rotational preference of the η^3-C_3H_5 group found in all but one[17] $MoX(CO)_2(\eta^3\text{-}C_3H_5)L_2$ (X = monodentate anion) complex. From an analogous isolobal treatment of an η^3-butadienyl fragment, it is apparent that for a suitable bonding interaction with this d^4 ML_5 fragment, the ligand will also bind as a substituted η^3-$C_3H_5^-$ moiety. An η^3-bonding mode has been noted in recent years in several butadienyl complexes, but none have had their bonding analyzed theoretically.[12,18-22]

The model complex used for these calculations is based on $Mo(CO)_2(\eta^3\text{-}CH_2C(CONHMe)C{=}CH_2)(bpy)(O_2CC_3F_7)$ (11), but in order to simplify the studies several approximations were made. This model complex, depicted in Figure 3, has been assumed to have a regular octahedral geometry as defined by the five ligands and the centroid of the η^3-allyl function. The allyl system itself is considered to be planar with the allyl plane lying perpendicular to the z axis of the complex. The 2,2'-bipyridine ligand was modeled as two coordinated ammonia molecules, the $O_2CC_3F_7$ ligand was truncated to O_2CCF_3, and the amide methyl group was treated as a proton. Interatomic distances and angles for the ligands and Mo–L separations were taken from the X-ray structure with idealized C–H and N–H distances of 1.10 and 1.01 Å, respectively. All calculations were performed by using Hoffmann's programs, which implement the standard extended Hückel molecular orbital (EHMO) method, as previously described.[1] Molybdenum parameters have been reported[1] and were used here also. Parameters for all other atoms are built into the program.

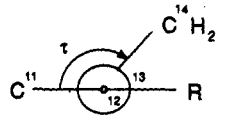

Figure 5. Torsion angle (τ) between the C(11)–C(12)–C(13) plane and the C(13)–C(14) vector.

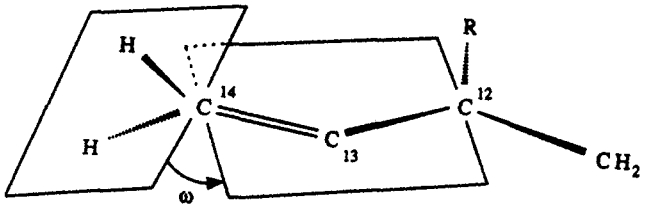

Figure 6. Torsion angle (ω) between the planes $H_2C(14)$ and C(12)–C(13)–C(14).

Table VII. Calculated Relative Energies for the η^3-Butadienyl Ligand

	rel energy, eV	
torsion angle (τ), deg	conjugated	unconjugated
180	+2.29	+1.19
90	+1.80	0

From the structure of $Mo(CO)_2(\eta^3\text{-}CH_2C(CONHMe)C{=}CH_2)(bpy)(O_2CC_3F_7)$, the bond angle of the η^3-butadienyl carbons C(12)–C(13)–C(14) (as defined in Figure 4) is 141.7° and the C(13)–C(14) bond length is 1.335 Å. The torsion angle C(11)–C(12)–C(13)–C(14) (τ) is defined as in Figure 5.

If τ is 180°, all four carbon atoms are coplanar in a trans arrangement. If the torsion angle τ is 90°, then the three allyl carbons C(11), C(12), and C(13) remain coplanar but C(14) is moved up out of this plane. Table VII presents the calculated relative energies at these two torsion angles of 180 and 90° with hydrogen positions chosen on C(14) corresponding to maximal and zero overlap between C(13) and C(14) pπ orbitals. These results show that for a given value of τ, the unconjugated arrangement is lower in energy than the conjugated arrangement by 1–2 eV. The overall lowest energy configuration by some 1.2 eV corresponds to a τ value of 90° and an unconjugated C(13)–C(14) π-bond. The preference for the unconjugated π-system is reflected in the calculated atomic charges. Thus for the coplanar arrangement with τ = 180°, the C(14) atom carries a charge of -0.12 for the unconjugated and -0.22 for the conjugated arrangement, and the Mo charge increases from 1.05 to 1.26. The conjugated arrangement is therefore doubly destabilized, as there is a weaker Mo–allyl interaction leading to a reduced charge donation from the ligand to Mo, and the build up of charge on C(14) occurs in the C(13)–C(14) antibonding π orbital.

A closer examination of the crystal structure of the butadienyl complex 11 revealed that this system showed a torsion angle of 125 (2)°, idealized to 120° for calculation purposes. With this value of τ it is not immediately obvious which positions of the hydrogen atoms on C(14) of the model relate to conjugated and unconjugated systems. A series of EHMO calculations were therefore undertaken in which the angle ω, defined as the angle between the planes containing carbon 14, its two hydrogen atoms, and C(12)–C(13)–C(14) (Figure 6), was altered in 10° incre-

(17) Brisdon, B. J.; Edwards, D. A.; Paddick, K. E.; Drew, M. G. B. *J. Chem. Soc., Dalton Trans.* **1980**, 1317.
(18) Hoberg, H.; Heger, G.; Krüger, C.; Tsay, Y.-H. *J. Organomet. Chem.* **1988**, *348*, 261.
(19) Bruce, M. I.; Liddell, M. J.; Snow, M. R.; Tiekink, E. R. T. *J. Organomet. Chem.* **1988**, *7*, 343. Bruce, M. I.; Hambley, T. W.; Liddell, M. J.; Snow, M. R.; Swincer, A. G.; Tiekink, E. R. T. *Organometallics* **1990**, *9*, 96.
(20) Guiliéri, F.; Benaim, J. *Nouv. J. Chem.* **1985**, *9*, 335.
(21) Nesmeyanov, A. N.; Kolobova, N. E.; Zlokina, I. B.; Lokshin, B. V.; Leshcheva, I. F.; Znobina, G. K.; Anisimov, K. N. *J. Organomet. Chem.* **1976**, *110*, 339.
(22) Bruce, M. I.; Hambley, M. R.; Snow, A. G.; Swincer, A. G. *Organometallics* **1985**, *4*, 494.

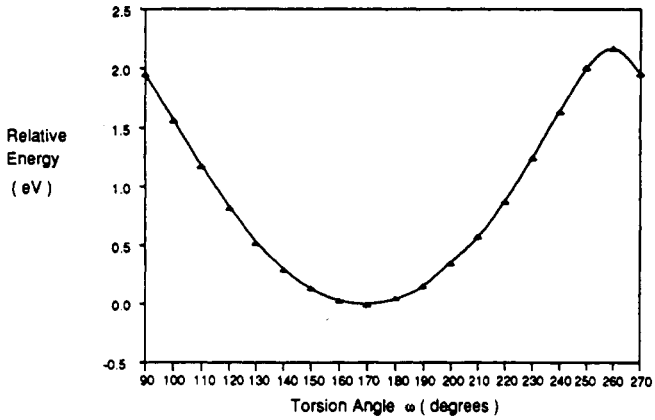

Figure 7. Calculated variation in relative energy of the model complex with torsion angle ω.

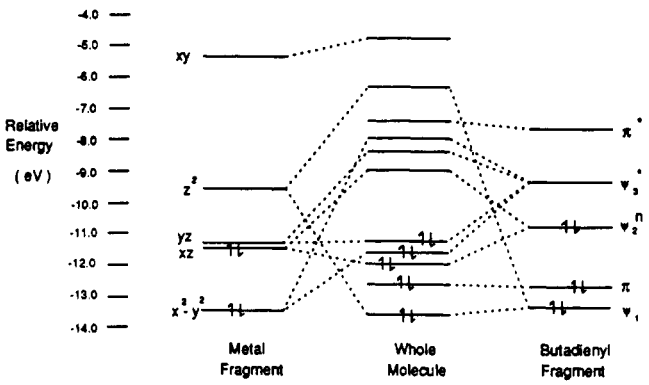

Figure 8. Fragment molecular orbital scheme for the model complex: EHMO interaction diagram between $Mo(CO)_2(NH_3)_2(O_2CCF_3)$ (left), $CH_2C(CONH_2)C{=}CH_2$ (right), and the whole complex (center).

ments. The total energy of the system was calculated for each increment as shown in Figure 7.

The minimum energy corresponds to an ω value of 170°. A model of **11** shows that this angle indicates an unconjugated system, and the calculations show that this is favored over a conjugated system by ca. 2.2 eV. When the arrangement of atoms that yields the lowest energy was established, a fragment molecular orbital analysis was carried out for the η^3-butadienyl and the $Mo(CO)_2(NH_3)_2(O_2CCF_3)$ fragments (Figure 8).

In the η^3-butadienyl fragment the bonding, nonbonding, and antibonding orbitals of the allyl functionality are essentially the same as for an unsubstituted allyl system. There is no significant contribution to these orbitals from either the amide group or the double bond of the η^3-butadienyl system. In addition to the three allyl orbitals there are also π-bonding and π^*-antibonding molecular orbitals corresponding to the double bond between carbons 13 and 14. These orbitals show no contribution from the allyl π-system. These features correlate with the double bond not being conjugated with the allyl π-system. The molecular orbitals of the metal fragment are essentially pure metal d orbitals. There is some evidence of orbital mixing with the carbonyl ligands, but this is not a significant effect. The energetic ordering of the metal fragment orbitals is as expected for such a species, with a π-acceptor role for the carbonyl ligands.

When the orbitals of the two fragments interact, the π and π^* functions of the double bond of the η^3-butadienyl system remain largely unchanged in energy and so play no significant part in the bonding of the two fragments. As a result, it is expected that this double bond will react in an independent sense toward nucleophiles and electrophiles. The d_{xy} orbital shows a slight destabilization, but does not appear to be involved in bonding to the η^3-butadienyl fragment. The energies of the remaining orbitals of the two fragments are all similar and so symmetry considerations are of greatest importance for interaction of the orbitals. The symmetric d_{z^2} orbital of the metal fragment forms bonding and antibonding combinations with the symmetric bonding orbital, ψ_1, of the allyl function of the η^3-butadienyl fragment. The bonding interaction is shown in Figure 9a. The d_{xz} metal fragment finds a symmetry match in the nonbonding allyl orbital, (ψ_2 Figure 9b), the antibonding combination giving rise to the lowest unoccupied molecular orbital (LUMO). The d_{yz} and, interestingly, the $d_{x^2-y^2}$ orbitals find a symmetry match in the antibonding allyl orbital, ψ_3^* (Figure 9c). The interaction of the $d_{x^2-y^2}$ and ψ_3^* orbitals does not give rise to a strongly bonding orbital and so does not affect the structure of this complex greatly. The interaction between d_{yz} and ψ_3^* also gives only a weakly bonding orbital, which forms the highest occupied molecular orbital (HOMO) of the complex. Since this bonding interaction is small, it also does not have a great influence on the structure of this complex. It has been reported however that many η^3-allyl complexes have structures in which the allyl group has a significant "nose-up" tilt.[13] This has been rationalized as being due to optimization of the overlap of the allyl ψ_3^* orbital with the d_{yz} orbital, the extent of the tilt depending upon the metal and the other ligands in the complex. In accordance with only a weak interaction of d_{yz} with ψ_3^*, complex **11** does not show a significant tilt angle.

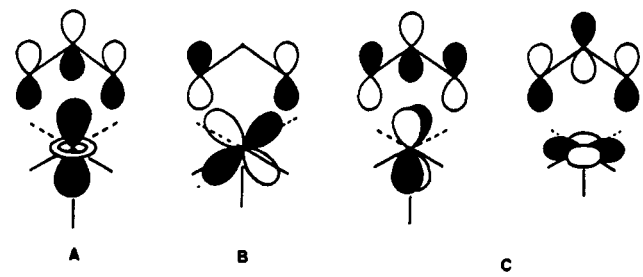

Figure 9. Metal d and ligand allyl type π orbital interactions for Mo-η^3-butadienyl coordination: (A) d_{z^2}–ψ_1 (bonding); (B) d_{xy}–ψ_2 (nonbonding); (C) d_{yz}, $d_{x^2-y^2}$–ψ_3 (antibonding).

Previous studies have shown that nucleophilic attack upon η^3-allyl complexes is frontier orbital (FMO) controlled.[1] The lowest energy acceptor orbital, the LUMO, in this model complex results from a combination of the d_{xz} orbital with the nonbonding ψ_2 orbital of the η^3-butadienyl fragment. Nucleophilic attack, if FMO controlled, would be directed toward the termini of the allyl function, i.e. C(11) and C(13) of the butadienyl system. Since this complex is asymmetric, the two termini of the allyl function are not equivalent and this asymmetry is reflected by the C(11) and C(13) p_z coefficients in the LUMO of 0.26 and -0.21, respectively. Nucleophilic attack would therefore be directed toward C(11), the position with the larger atomic coefficient in the LUMO and the least steric hindrance. This would yield an allene as shown in pathway a of Figure 10. In contrast, the charge distribution in the η^3-butadienyl ligand directs nucleophilic attack toward the carbon atom with the most positive net charge, in this case C(13), to yield a 1,3-butadiene. Given a reasonable FMO energy match between the amide complex and the attacking nucleophile, i.e. FMO control rather than charge control, then attack at C(11) is clearly indicated. The only example of nucleophilic attack on such a ligand that we are aware of involves the reaction of $Mo(CO)_2(\eta\text{-}C_5H_5)(\eta^3\text{-}CH_2C(CONEt_2)C{=}C(Me)(Ph))$ with $HNEt_2$.[20]

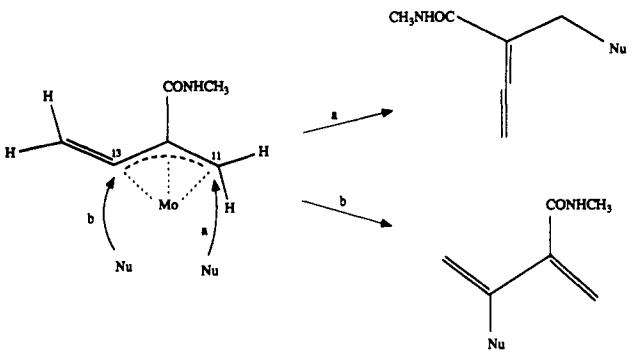

Figure 10. Products of nucleophilic attack at C(11) or C(13) of the η^3-butadienyl ligand.

The product $(\eta\text{-}C_5H_5)(CO)_2Mo(C(CONEt_2)(CH{=}C(Me)\text{-}Ph)CH_2NEt_2)$ conforms to these preceding predictions completely.

Electrophilic attack by H^+ upon a closely related complex, $Mo(CO)_2(\eta^3\text{-}CH_2CHC{=}CH_2)(\eta\text{-}C_5Me_5)$ has been recently reported[12] to occur at C(14), so yielding an η^3-vinylcarbene ligand. This unsubstituted η^3-butadienyl complex has been modeled by replacing the amide group of complex 11 with a hydrogen atom lying in the allyl plane, whilst all other features of the model complex have remained unchanged. If FMO controlled, electrophilic attack would occur at the carbon atom with the largest coefficient in the HOMO. In this model complex the HOMO is made up from a combination of d_{yz}, ψ_3*, and π* orbitals, the coefficients of greatest magnitude in the HOMO being 0.585 and 0.580 for C(12) and C(13), respectively. The magnitude of the coefficients for C(11) and C(14) are 0.480 and 0.447, respectively. Attack at C(14) is not indicated. If charge controlled, as is expected for protonation of such a complex where a large difference in frontier orbital energies exists, electrophilic attack will occur at the carbon atom with the most negative net charge, which in this unsubstituted η^3-butadienyl model complex is very clearly C(14) with a charge of -0.21, whilst the remaining carbon atoms have chanrges of -0.06, -0.11, and +0.08 for C(11), C(12), and C(13) respectively. Electrophilic attack on the amido model complex is also expected to occur at C(14) if charge controlled, but if FMO control predominates, then attack at C(11) is inferred from the coefficients of d_{yz} and ψ_3* orbitals, which make up the HOMO. The magnitude of the relative coefficients for C(11), C(12), C(13), and C(14) of the amido complex are 0.223, 0.195, 0.082, and 0.019, respectively, while the charges are -0.07, -0.05, -0.08, and -0.22 respectively.

A study was also undertaken of the orientation of the methylamido group on C(12), for which the *E* conformation is observed crystallographically (Figure 11a). The atomic charges computed for both *Z* and *E* conformers indicate that the *E* conformation would lead to favorable attractive electrostatic interactions, which would be repulsive in the *Z* form, in which there is an additional unfavorable H–H contact of ~1.7 Å (Figure 11b). However, the EHMO total energies for the two isomers differ by less than 0.05 eV. This is because electrostatic interactions are not explicitly incorporated into the EHMO treatment. Moreover, the unfavorable H–H contact, while antibonding, does not lead to a large enough overlap to influence the total energies significantly. This is not surprising, since the H 1s orbital exponent is better matched to modeling short-range covalent interactions than long-range nonbonded contacts. The latter can be partially accounted for by reducing the 1s exponents of the relevant H atoms. For a ξ value of 1.0 the *Z* arrangement is indeed found to be 0.1 eV higher in

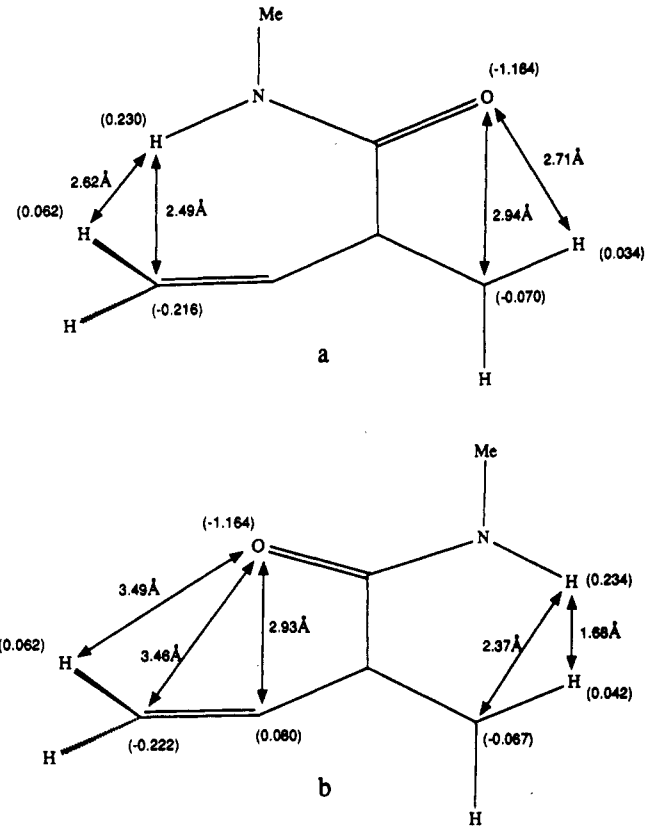

Figure 11. Close contacts within the (a) *E* and (b) *Z* conformations of the (methylamido)butadienyl ligand. Atomic charges are given in parentheses.

energy than the *E* conformation, but it is clear that a more elaborate treatment than simple EHMO theory is required to describe nonbonded interactions effectively.

Conclusion

On the basis of the structural and spectroscopic properties described above and the results of the EHMO analysis, we consider that these complexes may best be regarded as η^3(3e)-buta-2,3-dienyl derivatives, in which the uncoordinated carbon–carbon double bond remains unconjugated with respect to the π-delocalization within the η^3-allyl fragment. A contribution from a zwitterionic form such as A, in which the butadienyl ligand acts as a 4-

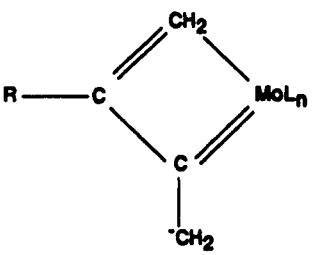

A

electron source and introduces some double-bond character into the Mo–C(13) link, accounts for the ^{13}C chemical shift of C(13) (ca. 165 ppm) and the close approach of these two atoms to a distance of 2.200 (10) Å, which is intermediate between values typifying Mo–C bond orders of 1 and 2.[23]

(23) Allen, S. R.; Beevor, R. G.; Green, M.; Norman, N. C.; Orpen, A. C.; Williams, I. D. *J. Chem. Soc., Dalton Trans.* **1985**, 435.

Experimental Section

The starting materials $Ph_4P[MoCl(CO)_3L_2]$ (L_2 = 2,2'-bipyridyl, 1,10-phenanthroline) were prepared from $Mo(CO)_4L_2$ and Ph_4PCl by using procedures described previously.[7] Solvents were dried over molecular sieve 4A prior to use; other reactants were used as received from commercial sources. All reactions were carried out under an atmosphere of dry dinitrogen gas. Infrared spectra were recorded as paraffin mulls on a Perkin-Elmer 599B spectrometer, and NMR spectra were obtained by using a JEOL GX 270 MHz FT instrument with samples dissolved in CD_2Cl_2 and TMS as an internal standard. The Raman spectrum of solid **10** was recorded by using a Spex 1401 spectrometer in conjunction with a Lexel argon ion laser. Elemental analyses were carried out by the Analytical Services, University of Bath.

Preparation of $MoCl(CO)_2(\eta^3\text{-}CH_2C(CONRR')C{=}CH_2)L_2$ (L_2 = bpy, R = H, R' = Me, Et, Pr^n, Ph, $CH_2CH{=}CH_2$, $CH_2C{\equiv}CH$; R = R' = Me, Et, Pr^n; L_2 = phen, R = R' = Et). The conditions and reaction times involved in the synthesis of these complexes were dependent upon the nature of the amine involved. The same basic procedure was used, but the amines could be classified into two groups, A and B, depending upon which one of two solvent mixtures was required. The general method of preparation is given below, and the amines are allocated to groups A or B in Table I.

A suspension of $Ph_4P[MoCl(CO)_3L_2]$ (1.0 mmol) in the required solvent mixture (1:1 dry, deoxygenated MeOH and THF (10 mL) for amines in group A, or methanol (10 mL) and water (0.5 mL) for amines in group B) was stirred with excess amine RR'NH (0.5 mL) at -10 °C. To this suspension was added dropwise 1,4-dichlorobut-2-yne (0.15 mL, 1.0 mmol), and the temperature maintained at -10 °C for 0.5 h. When the mixture was warmed to room temperature and stirred for a further 0.5 h (group A) or 1.5 h (group B), a deep red solution was produced. This was reduced in volume in vacuo to ca. 5 mL and 40–60 °C petroleum ether (5 mL) was added to the filtered solution. On storage at -10 °C, the products were isolated as orange, microcrystalline products and the more soluble complexes were recrystallized from CH_2Cl_2–petroleum ether mixtures. Analytical data and yields are given in Table I.

Preparation of $Mo(CO)_2(\eta^3\text{-}CH_2C(CONHR')C{=}CH_2)(bpy)(O_2CC_3F_7)$ (R' = Me, Et, Pr^n, Ph, $CH_2CH{=}CH_2$). A solution of silver tetrafluoroborate (0.2 g, 1.0 mmol) in acetone (5 mL) was added dropwise to a mixture of excess sodium heptafluorobutyrate (250 mg) and $MoCl(CO)_2(\eta^3\text{-}CH_2C(CONHR')C{=}CH_2)bpy$ (1.0 mmol) in acetone (10 mL) and the reaction mixture stirred at room temperature for 3 h. The orange filtered solution was reduced to ca. 5 mL in vacuo and added dropwise to stirred petroleum ether (50 mL). The precipitated products were isolated as orange or yellow microcrystalline powders. Several recrystallizations from CH_2Cl_2–petroleum ether mixtures were necessary to remove traces of inorganic salts. Yields and analytical data are given in Table I.

Competition Experiments. Reactions between $[MoCl(CO)_3bpy]^-$ and $ClCH_2C{\equiv}CCH_2Cl$ in the presence of methanolic solutions of equal volumes (0.5 mL) of two amines were carried out by using the method described for group A complexes. Only one major product could be isolated from each reaction.

Structure Determination. A single crystal of **11** (0.5 × 0.4 × 0.15 mm) was grown from a CH_2Cl_2–petroleum ether mixture, coated in epoxy resin, and mounted on a Hilger and Watts Y290 automatic four-circle diffractometer. Unit cell dimensions (Table IV) were determined by least-squares refinement of the best angular positions for 12 independent reflections ($\theta > 12°$) using graphite-monochromated molybdenum radiation (λ = 0.710 69 Å). A total of 3355 reflections were collected at room temperature in the range $2 \leq \theta \leq 22°$, of which 2296 were unique with $I \geq 3\sigma(I)$. A standard reflection was monitored every 90 min during data collection and showed no significant variation in intensity. Data were corrected for Lorentz and polarization effects but not for absorption. The structure was solved by conventional direct methods using the SHELX[24,25] suite of programs. In the final stages of convergence all atoms except for carbons 1–10 (of the bpy ligand) and C(21) were allowed to vibrate anisotropically. Hydrogen atoms were included at calculated positions on the relevant atoms except for the butadienyl carbons [C(11)–C(14)]. Final residuals after 14 cycles of full-matrix least-squares refinement were R = 6.38%, R_w = 7.23% for a weighting scheme of $w = 3.0065/[\sigma^2(F_o) + 0.0010(F_o)^2]$. The total number of parameters varied was 288. Max final shift/esd was 0.02, average = 0.004. Maximum and minimum residual densities were 0.41 and -0.46 e Å^{-3}, respectively, in the region of the metal and as such bear no chemical significance. Scattering factors and anomalous dispersion corrections were taken from ref 26.

Acknowledgment. We thank the SERC for a studentship (C.M.K.).

Supplementary Material Available: Tables of fractional atomic coordinates for the hydrogen atoms, anisotropic thermal parameters, and bond lengths and angles (5 pages); a listing of observed and calculated structure factors (13 pages). Ordering information is given on any current masthead page.

(24) Sheldrick, G. M. SHELX86, Program for Crystal Structure Determination, University of Göttingen, Federal Republic of Germany, 1986.
(25) Sheldrick, G. M. SHELX76, Program for Crystal Structure Determination, University of Cambridge, UK, 1976.
(26) *International Tables for X-Ray Crystallography*; Kynoch Press: Birmingham, U.K., 1974; Vol. 4.